Bioelectromagnetics 6:243–256 (1985)

The Extremely Low Frequency Electrical Properties of Plant Stems

Francis X. Hart

Department of Physics, University of the South, Sewanee, Tennessee

The electrical properties (variation of capacitance and conductance with frequency) of a plant stem can be conveniently measured in vivo by time domain dielectric spectroscopy. In this technique a voltage step is applied to a stem. The resulting polarization current is sampled by a microprocessor and Fourier-transformed to yield these properties. Spectra were obtained for seven electrode separations along a Poinsettia stem. The inverse capacitance and conductance were plotted vs separation for 50 frequencies from .35 to 350 Hz. Least-square fits yielded the effective dielectric constant and conductivity of the stem over this frequency range. In this way electrode effects were eliminated. A similar procedure was carried out for Coleus.

A log-log plot of dielectric constant vs frequency shows a two-stage linear decrease for both plants. The conductivity is primarily DC. The dielectric loss decreases smoothly with frequency for Coleus. These results are compared to those for bone and the inorganic material hollandite. The dielectric properties seem best described by a cooperative, many-body approach.

Key words: **electrical, dielectric, capacitance, conductance, impedance, plant stems**

INTRODUCTION

Knowledge of the electrical properties of biomaterials is important for several reasons. The calculation of the internal fields produced by external sources depends on the values used for the dielectric constant and conductivity of the tissue at the frequency of exposure. The practical application of impedance measurements to monitor physiological changes as diverse as the ripening of avocados [Bean et al, 1960], the onset of estrus in cows [Edwards, 1980], and the repair of plant stems [Hart, 1982b] can be optimized by determining the frequencies at which these changes are most pronounced. Finally, comparison of the electrical properties of biomaterials with each other and with inorganic materials can lead to a better understanding of the basic conduction and polarization processes in these materials and perhaps to an understanding of the origin of nonthermal electromagnetic bioeffects.

Two major problems are associated with the measurement of the extremely low frequency (ELF) electrical properties of biomaterials. First, a realistic description of the properties of living systems requires in vivo measurements. Unfortunately, ordinary bridge techniques can be time-consuming. The physiological state of the system and thus the associated electrical properties can be changing during the course of the

Received for review November 28, 1983; revision received October 19, 1984.

Address reprint requests to Francis X. Hart, Department of Physics, University of the South, Sewanee, TN 37375.

measurements. Second, the contribution of the electrodes must be separated from that of the tissue under study.

The present paper describes a system which uses time domain dielectric spectroscopy (TDDS) to rapidly measure, in vivo, the ELF electrical properties of plant stems. Broadhurst [1970] has reported the radio frequency and microwave properties of leaves and branches for a variety of plants. In TDDS a voltage step is applied to a stem. The resulting current is sampled and stored under microprocessor control. Fourier transformation yields the corresponding variation of capacitance and conductance with frequency. In this paper a least-squares fitting procedure is then applied to the results for several electrode separations. Electrode effects are eliminated, and values for the dielectric constant and conductivity of the stem itself are obtained over a wide range of frequencies. Although the method is described here for plant stems, it is applicable to a wide variety of biomaterials, such as bone.

PROCEDURE

The details of the basic apparatus and procedures in the applications of TDDS are described elsewhere [Singh et al, 1979; Hart, 1982a,b, 1983a,b, 1984]. Several points should be emphasized here. Two parallel RC combinations connected in series can serve as a test material for the accuracy and sensitivity of the TDDS system. The measured frequency variation of its capacitance and conductance can be compared with the results predicted from theory. Very good agreement is obtained if the sampling resistance is small in comparison with the test impedance [Hart, 1982a].

For a fixed electrode spacing the shape of the current-time response remains essentially unchanged for days. Varying moisture content translates the curve up or down, but does not affect its overall shape. In fact, the healing of a slit stem can be followed by monitoring the gradual return of the current-time response to its original shape prior to slitting [Hart, 1982b]. Little variation in shape is observed for the same separation with different plants of the same species.

In the present study a series of stainless steel sewing pins (radius .5 mm) was inserted in the upper, herbaceous part of a Poinsettia stem. Used in different combinations these pins provided a variety of electrode separations (d). The insertion of pins into plant stems produces localized damage. Long-term monitoring of the interelectrode potential indicates, however, that the perturbation lasts at most 50 h [Gensler, 1974]. Similar measurements made on the plants used in this study confirmed these results. As a precaution, several days were allowed after insertion for the pins to come into equilibrium with the surrounding tissue before the experiment was begun.

A 9-volt step was applied to a given pair of electrodes at $t = 0$. The resulting current was sampled at 1-msec intervals for 3 sec. This procedure was carried out for seven different sets of electrode pairs with separations ranging from .006 to .137 m. One of these seven measurements repeated a previous electrode separation (.031 m) with a different pair of pins as a check on the consistency of the results. Successive runs were made at 15-min intervals. This time period was long enough that the perturbation to the next current-time response was small, yet short enough that the physiological state of the plant would not change during the entire series of measurements.

The current passing through the stem has the form

$$i(t) = i_o(t) + i_p(t) + i_{DC} \tag{1}$$

where $i_o(t)$ is an initial transient before the first measuring interval associated with the charging of the system's high-frequency capacitance, $i_p(t)$ is the polarization current, and i_{DC} is the steady-state conduction current [Hart, 1982a]. Most dielectrics are observed to obey the Curie–Von Schweidler law

$$i_p(t) = A\, t^{-n} \tag{2}$$

in a series of one or more stages. A and n are parameters which depend on the system under study.

RESULTS

Figure 1 illustrates the two-stage decrease of the current with time for an intermediate electrode separation. Three thousand current readings were taken, but only about 100 are shown for clarity. Note the greatly expanded current scale. On a log-log plot equation 2 is a straight line with slope −n. If t is measured in milliseconds, then A is the intercept. The two n values were obtained from a least-squares fit. The discrete changes in the digitized current values are evident.

Figure 2 compares the results for three of the electrode separations. As the separation increases, the magnitude of the current decreases, and the overall slope is lower. The two-stage linear dependence for the .031-m separation is not apparent on this scale, as it is on the expanded scale of Figure 1. Curve 1 displays two clear linear, decreasing stages followed by an anomalous increase for $t > 2{,}500$ msec. Although only a few points are shown in the figure for this region, several hundred current measurements were made during this time interval. Hence the rise is real and not an artifact. A similar increase was also observed at the next shortest electrode separation.

For five of the seven separations the current was observed to decrease in two sequential Curie–Von Schweidler stages

$$\begin{aligned} i(t) &= A_1 t^{-n_1} \text{ for } 1 \text{ ms} \leqslant t \leqslant t_1 \\ i(t) &= A_2 t^{-n_2} \text{ for } t_1 \leqslant t \leqslant t_2. \end{aligned} \tag{3}$$

For each separation A_1, A_2, n_1, and n_2 were found by a least-squares fit. Table 1 summarizes the results. In several cases it appeared that the data might be adequately fit by a single straight line. For each of the seven electrode separations the square of the correlation coefficient, r^2, was calculated for both a single and a double straight line fit [Kirk, 1978]. The result with the higher r^2 value is presented in Table 1. The r^2 values typically were greater than .95. Only one straight line was required for the .093- and .137-m separations. Note also that the two results for d = .031 m are in

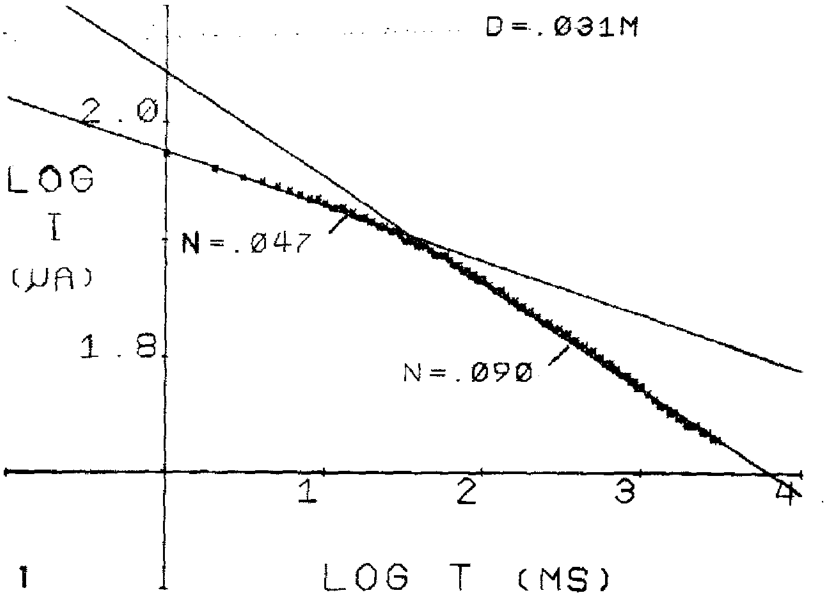

1

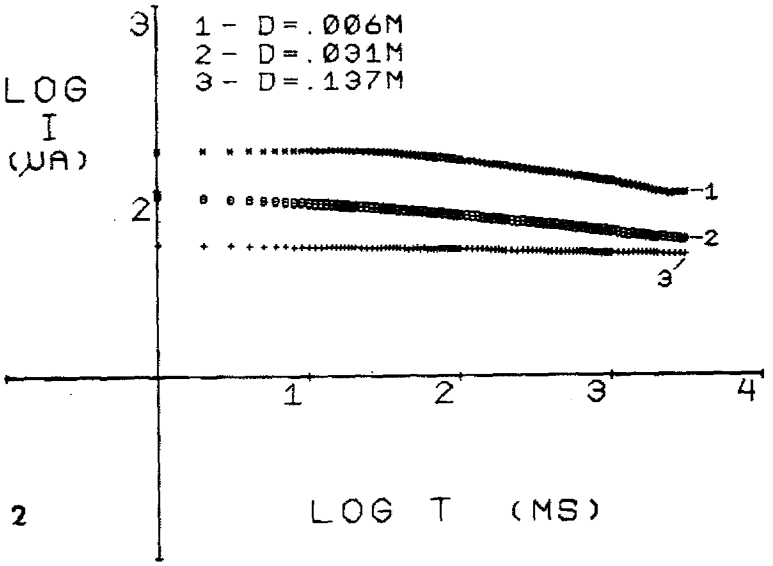

2

Fig. 1. Variation of the polarization current in Poinsettia with time for an electrode separation of .031 m. Current is in microamperes, time in milliseconds. The ordinate scale is logarithmic.

Fig. 2. Comparison of the polarization currents in Poinsettia for three electrode separations (d): curve 1 (*), d = .006 m; curve 2 (O), d = .031 m; curve 3 (+), d = .137 m. The ordinate scale is logarithmic.

TABLE 1. Polarization Current Parameters for Several Electrode Separations

Electrode separation (d(m))	A_1 (μA)	n_1	t_1 (msec)	A_2 (μA)	n_2	t_2 (msec)
.006	166	0	17	239	.11	2,500[a]
.018	118	.038	30	131	.070	2,500[a]
.031	115	.035	25	125	.060	3,000
.031	94.5	.047	30	110	.090	3,000
.050	83.0	.036	40	91.2	.060	3,000
.093	57.2	.034	3,000	—	—	—
.137	51.9	.020	3,000	—	—	—

[a] Anomalous current increase appears.

relatively good agreement. The curves have similar shapes, but are separated by about 15–20 μA. In each case $n_2 > n_1$ and $A_2 > A_1$. Both A_1 and A_2 decrease steadily with d, as expected. It should be emphasized that the overall results of this experiment do not depend in any way on the goodness of these fits. The original, digitized data are used in the following numerical calculations of capacitance, C(f), and conductance, G(f).

The overall current-time response is determined by contributions from the electrodes and from the stem itself. As the electrode separation increases, the latter becomes relatively more important. The changes in the response indicated in Table 1 reflect the decreasing importance of the electrodes as the separation increases.

The capacitance C and conductance G of the region between the electrodes are given as functions of frequency f by

$$C(f) = C_H + V^{-1} \int_{\text{T-Min}}^{\text{T-Max}} (i(t) - i_{DC}) \cos(2\pi ft)\, dt \tag{4}$$

and

$$G(f) = V^{-1} i_{DC} + 2\pi f V^{-1} \int_{\text{T-Min}}^{\text{T-Max}} (i(t) - i_{DC}) \sin(2\pi ft)\, dt \tag{5}$$

where C_H is the high-frequency capacitance and V is the amplitude of the voltage step [Hart, 1982a]. T-Min and T-Max are the times at which the current was initially and finally sampled (.001 sec and 3 sec). The frequency range is then $1/\text{T-Max} \leqslant f \leqslant 1/2\text{T-Min}$. Note that only the polarization current $(i(t) - i_{DC})$ appears in the integrands. i_{DC} determines the steady-state conductance through the $V^{-1}i_{DC}$ term, but does not affect the frequency dependence of G(f) or C(f). Hence simple translations in the amplitude of the current-time response do not affect the changes in conductance and capacitance with frequency.

Figures 3 and 4 illustrate the capacitance and conductance spectra corresponding to the three currents of Figure 2. Although the current curves are relatively smooth, the transformed spectra, especially C(f), contain time-varying noise at high frequencies. This noise originates in the use of a finite time window and the discrete changes in the digitized current which yield waves upon transformation. The actual C(f) and G(f) curves should be drawn smoothly through the scattered points.

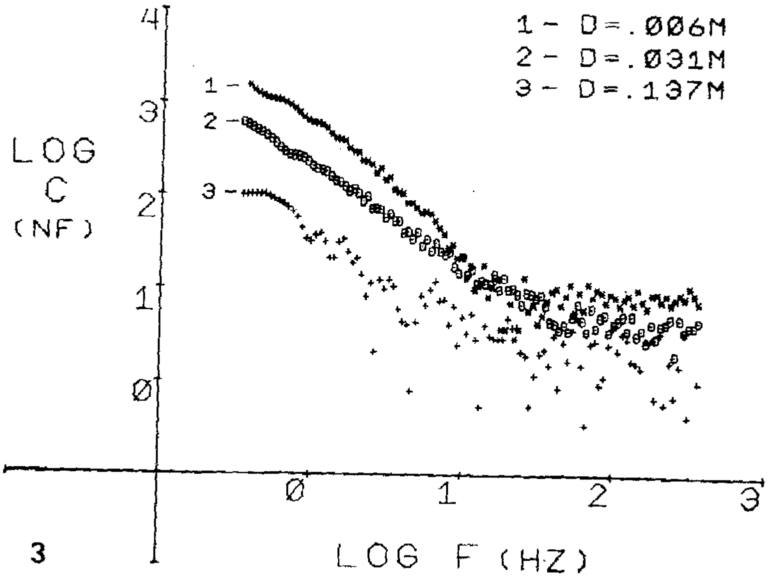

3

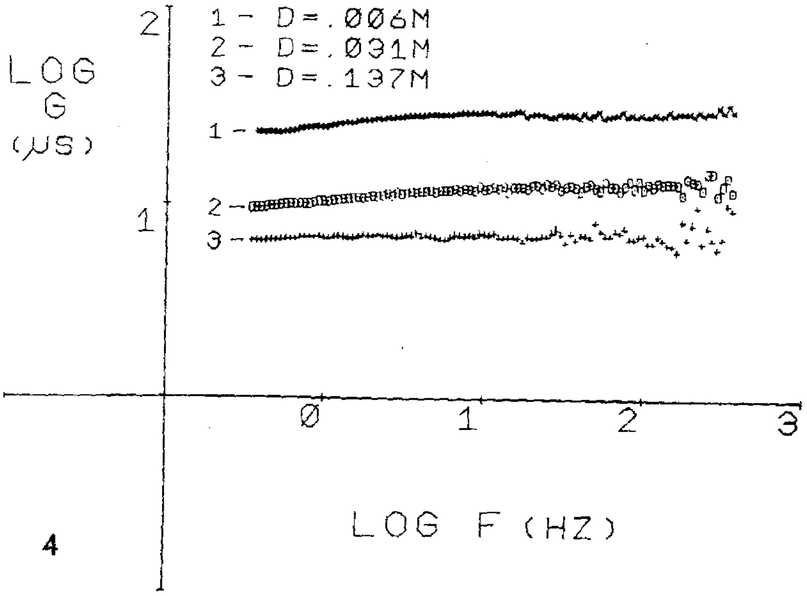

4

Fig. 3. Capacitance spectra corresponding to the three currents of Figure 2. Capacitance is in nanofarads, frequency in Hertz. The ordinate scale is logarithmic.

Fig. 4. Conductance spectra corresponding to the three currents of Figure 2. Conductance is in microsiemens, frequency in Hertz. The ordinate scale is logarithmic.

The interelectrode capacitance C may be regarded as the series combination of an electrode capacitance C_e and the capacitance of the stem itself which is $K\epsilon_0 S/d$. S is the cross-sectional area of the stem, K is its dielectric constant and ϵ_0 is the permittivity of free space. Thus

$$C^{-1} = C_e^{-1} + d/K\epsilon_0 S. \tag{6}$$

Similarly for the conductance

$$G^{-1} = G_e^{-1} + d/\sigma S \tag{7}$$

where G_e is the electrode conductance and σ is the conductivity of the stem. Equations 6 and 7 assume that the interelectrode material is homogeneous; the resulting permittivity and conductivity values thus represent averages over the entire stem. Any nonuniformities in the current distribution near the electrodes are neglected as well.

At any one frequency a plot of C^{-1} vs d should be a straight line whose slope yields the dielectric constant of the stem at that frequency. Similarly, the conductivity of the stem is found from the slope of a plot of G^{-1} vs d. Values of C and G were taken from the smoothed C(f) and G(f) curves for the seven electrode separations at 52 frequencies from .35 to 350 Hz. For each frequency C^{-1} was plotted vs d. A least-squares linear fit was made and K then determined from its slope. In the same way G^{-1} was plotted vs d for each of the 52 frequencies, and σ was determined from the slope of a linear least-squares fit. The cross-sectional area S varied somewhat over the full 14-cm stem length. An average value of 1.2×10^{-5} m^2 was used to find K and σ. Figures 5 and 6 illustrate the fits for 1, 10, and 100 Hz. The large differences in the slopes of the C^{-1} vs d curves imply a strong dependence of dielectric constant on frequency, whereas the small difference in the slopes of the G^{-1} vs d curves indicate a weak dependence of conductivity on frequency.

A similar procedure was carried out for an upper Coleus stem. The same basic pattern was observed as for Poinsettia. The n values for the currents were closer to zero. The wavy high-frequency noise was relatively more important, but i_{DC} decreased more smoothly with increased electrode separation.

The C^{-1} values for large separations could be in error by perhaps 25% at high and intermediate frequencies because of the need to smooth the wavy high-frequency noise. For medium and small separations the error is at most 10% at high frequencies. The G^{-1} values are dominated by the DC contribution. The wavy noise is less important, and relatively little smoothing is necessary.

The two independent measures of the current-time response for the .031-m separation can also be used to obtain an indication of the error in the C^{-1} and G^{-1} values. The responses differ mainly in amplitude rather than in time dependence. The smoothed curves of C(f), which depends primarily on $i(t) - i_{DC}$, are thus indistinguishable for these two. The smoothed curves of G(f), which depends primarily on $V^{-1}i_{DC}$, are nearly parallel, but separated by about 25%. The points for the two sets of .031-m separations are thus coincident in Figure 5, but differ by about 25% in Figure 6. The error bars in Figure 5 represent the uncertainty in the C^{-1} values due to smoothing whereas those in Figure 6 represent the uncertainty in the G^{-1} values due to nonrepeatability.

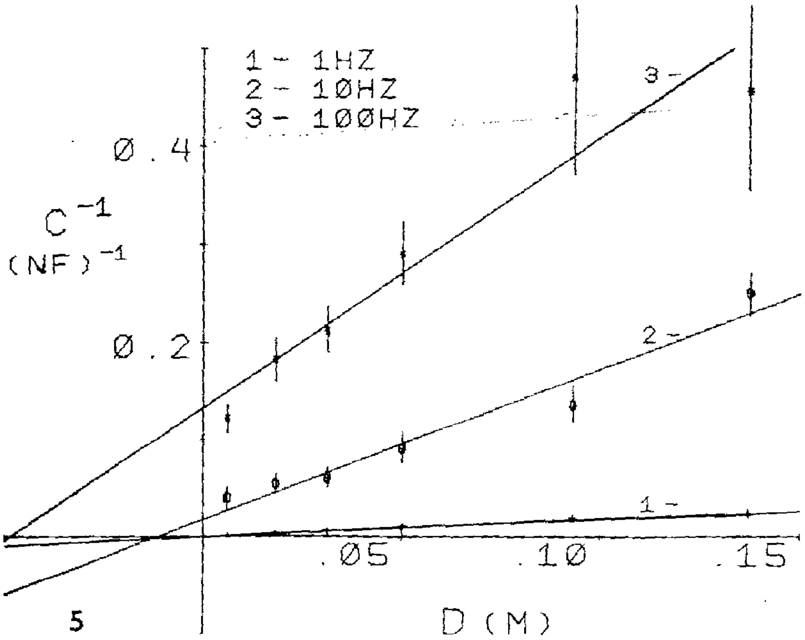

5

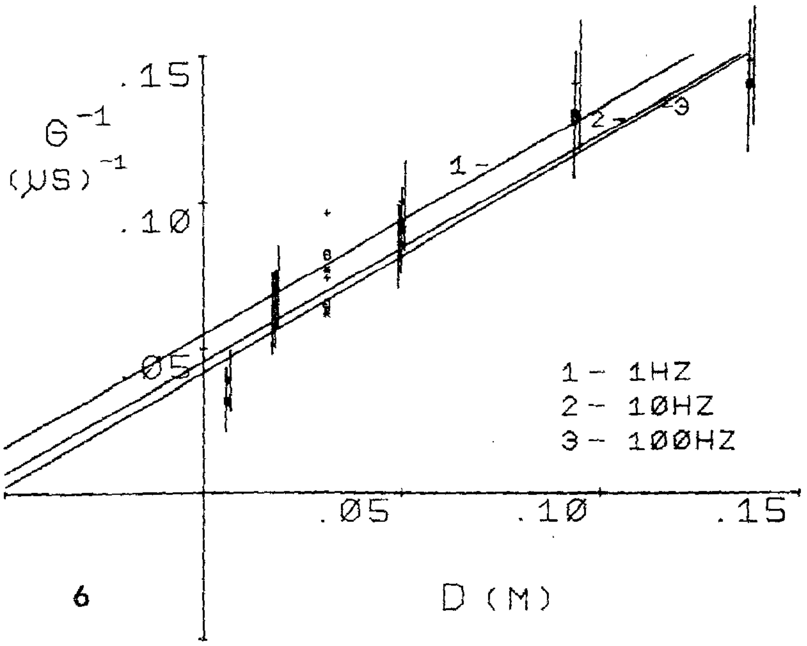

6

Fig. 5. Reciprocal capacitance in nanofarads vs electrode separation in meters for three frequencies: curve 1 (+), f = 1 Hz; curve 2 (O), f = 10 Hz; curve 3 (*), f = 100 Hz. The lines are least-squares fits to the data. The ordinate scale is linear.

Fig. 6. Reciprocal conductance in microsiemens vs electrode separations in meters for the same frequencies as in Figure 5.

Equations 6 and 7 assume that the electrode capacitance and conductance are the same for each pair of electrodes and that the interelectrode material is homogeneous and of constant cross section. Extrapolation of the lines in Figures 5 and 6 to d = 0 provides an estimate for the relative importance of C_e^{-1} and G_e^{-1}. The intercepts for the C^{-1} lines are less than about one-fourth the maximum values. The intercepts for the G^{-1} lines are less than about one-third the maximum values. Small variations in electrode capacitance and conductance should not greatly affect the slopes, which determine K and σ. The error should, however, be more significant for σ than for K.

Care was taken to select a stem segment that contained no branches. Conduction pathways should have been continuous. The cross section of the Poinsettia stem was not exactly circular, nor was the Coleus cross section exactly square. The error introduced by this geometrical "smoothing" and any irregularities in the cross section certainly did not exceed 10% for S.

A different measure of the overall error can be obtained by examining the r^2 values associated with the fitting procedures. The C^{-1} fits for Poinsettia have $r^2 \geqslant .95$ for $80\text{ Hz} \geqslant f \geqslant .4\text{ Hz}$. r^2 drops to .90 by 100 Hz and to .61 at 350 Hz. For Coleus $r^2 > .8$ for $250\text{ Hz} \geqslant f \geqslant .6\text{ Hz}$. Below .6 Hz and above 250 Hz the fits are poor. The G^{-1} fits for Poinsettia have $.95 \geqslant r^2 \geqslant .85$ for all frequencies. For Coleus $r^2 > .8$ for $f \leqslant 10\text{ Hz}$ and $r^2 > .75$ for $f > 10\text{ Hz}$. The fitting error is a combination of the errors in homogeneity, equivalence of electrodes, smoothing, and repeatability. As a conservative estimate the overall error range in K and σ is taken to be on the order of 25%.

It could be argued that the relatively large amplitude of the voltage step might generate ions because of electrolysis. The subsequent propagation of these ions through the stem would modify its measured electrical properties. However, the application of a 9-volt, 3-sec step has been shown [Hart, 1983a] to increase overall stem conductance by about 5%, which is small in comparison to the above uncertainties.

Figure 7 shows the resulting variation of dielectric constant with frequency for Poinsettia and Coleus. For both plants two linear stages are apparent in this log-log plot. Their dielectric constants can thus be expressed as

$$\begin{aligned} K(f) &= K_1 f^{-p_1} \text{ for } .35\text{ Hz} \leqslant f \leqslant f_1 \\ K(f) &= K_2 f^{-p_2} \text{ for } f_1 \leqslant f \leqslant 350\text{ Hz}. \end{aligned} \tag{8}$$

Values for K_1, K_2, p_1, and p_2 were obtained from a least-squares fit. For Poinsettia $K_1 = 5 \times 10^7$, $p_1 = 1.2$ with $r^2 = .99$ and $K_2 = 1 \times 10^7$, $p_2 = .3$ with $r^2 = .99$. For Coleus $K_1 = 8 \times 10^7$, $p_1 = 2.1$ with $r^2 = .96$ and $K_2 = 1 \times 10^7$, $p_2 = .6$ with $r^2 = .99$.

Figure 8 shows the variation of conductivity with frequency for Poinsettia and Coleus. The slight overall increase for Coleus and perhaps Poinsettia is well within the error bars. It should be recalled, however, that the conductivity error is determined primarily by the lack of reproducibility of i_{DC}. For every individual electrode separation for both Coleus and Poinsettia G(f) increased slightly with frequency. Although the baseline σ values may have significant error, the increase with frequency is real. The increase for Poinsettia is obscured by the scattering of points at low frequencies. It may seem odd that the σ increase is clearer for Coleus, which had the greater wavy noise. Recall, however, that the wavy noise appeared at high frequencies and was more important for C(f) than G(f). The greater scatter at low frequencies here for Poinsettia is due to the less consistent variation of i_{DC} with electrode separation.

For Coleus the total conductivity can be expressed as the sum of a steady-state term σ_o and a term which varies with frequency σ_{AC}. Thus $\sigma = \sigma_o + \sigma_{AC}$. Because conductivity was still decreasing slowly at the lowest frequencies, it is clear that a steady state had not been reached. This observation is confirmed by noting that the current was still decreasing at T-Max for the longer electrode separations. As a rough estimate we may take $\sigma_o = \sigma$ (f = .35). Approximate values can then be obtained at the remaining frequencies. The error introduced by this approximation is greatest at the frequencies closest to .35 Hz. Hence this step was omitted for the lowest frequencies. The results are shown in Figure 9. The dielectric loss Γ (f) = $\sigma_{AC}/2\pi f\epsilon_o$, plotted in Figure 10, decreases smoothly with frequency with no peak apparent. It must be emphasized that these curves, being based on the identification of σ_o with the lowest experimentally determined conductivity, can only be used to identify general trends.

Current-time responses were obtained for two Coleus and two Poinsettia plants with the same electrode separations. The current values for the Poinsettia agreed within about 10%. Similar results were obtained for Coleus. Such agreement is fortuitous in that varying moisture content can translate the response curve for a single plant up and down by ± 15% over a period of 3 weeks [Hart, 1982b]. The shape, however, is unaffected. A general comparison of the variation in stem dielectric properties within a species has yet to be performed. Work in progress on Schefflera stems indicates that the variation in current-time response shape with differing step amplitude is reproducible across plants if moisture is carefully controlled. With regard to the present study the absolute values for K and σ may perhaps vary by ± 25% between comparable plants and by ± 20% for a single plant depending on the environmental conditions. The overall frequency dependence, however, should not change.

DISCUSSION

Only the most general conclusions can be drawn from these results. The dielectric properties of Coleus and Poinsettia stems are not independent of frequency in the range 350 Hz $\geqslant$ f $\geqslant$ 0.35 Hz. For each plant the dielectric constant exhibits a two-stage power law decrease with frequency. The conductivity results are far more uncertain. A slight increase in conductivity corresponding to a featureless decrease of dielectric loss can be detected for Coleus.

The low frequency dispersion apparent in Figure 7 could be regarded as simply a continuous distribution of Debye-type relaxations. It is difficult to understand, however, why the distribution should always be such as to produce the generally observed f^{-p} frequency (t^{-n} current) dependence. A cooperative, many-body response model [Dissado and Hill, 1979; Ngai and White, 1979; Jonscher, 1981; Young, 1982] which obtains the f^{-p} frequency (t^{-n} current) behavior from first principles seems preferable. In such models the low-frequency dispersion is produced by correlations among charge carriers and their coupling with their surroundings.

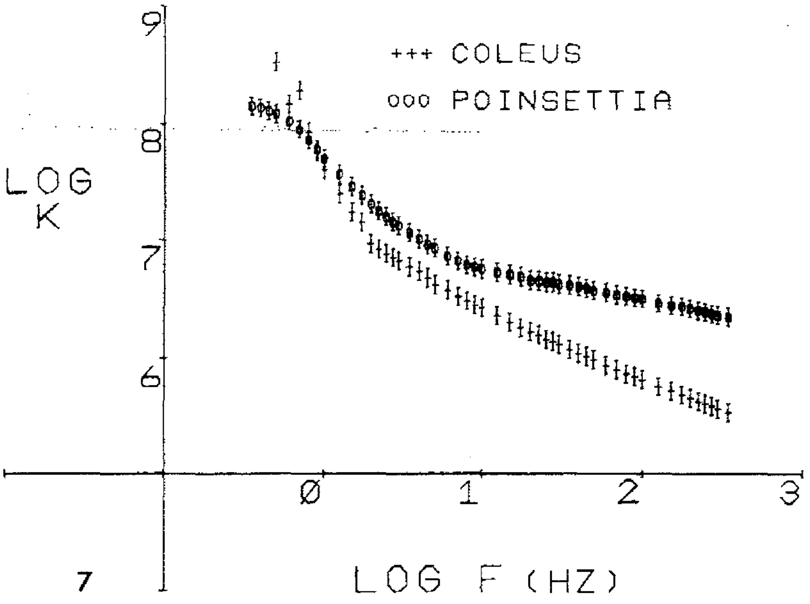

7

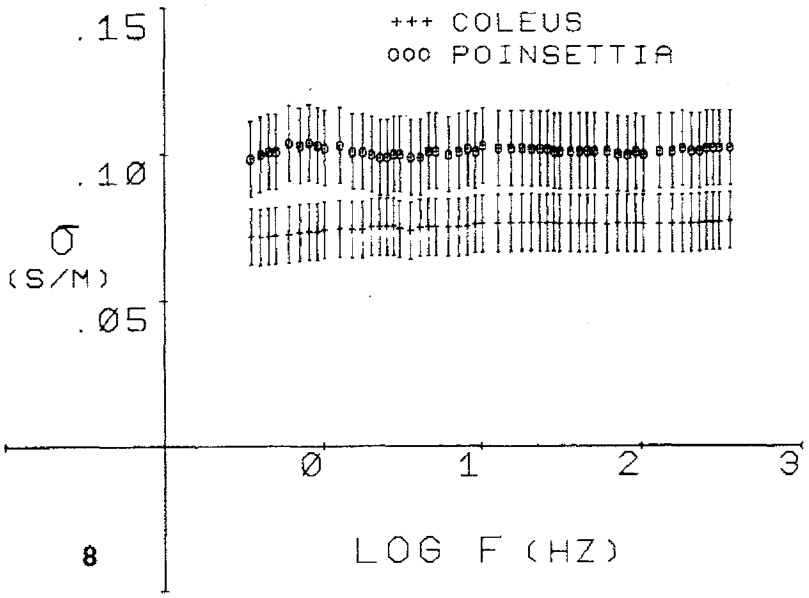

8

Fig. 7. Variation of stem dielectric constant with frequency in Hz for Coleus (+) and Poinsettia (O). The ordinate scale is logarithmic.

Fig. 8. Variation of stem total conductivity in Siemens/m with frequency in Hz for Coleus (+) and Poinsettia (O). The ordinate scale is linear.

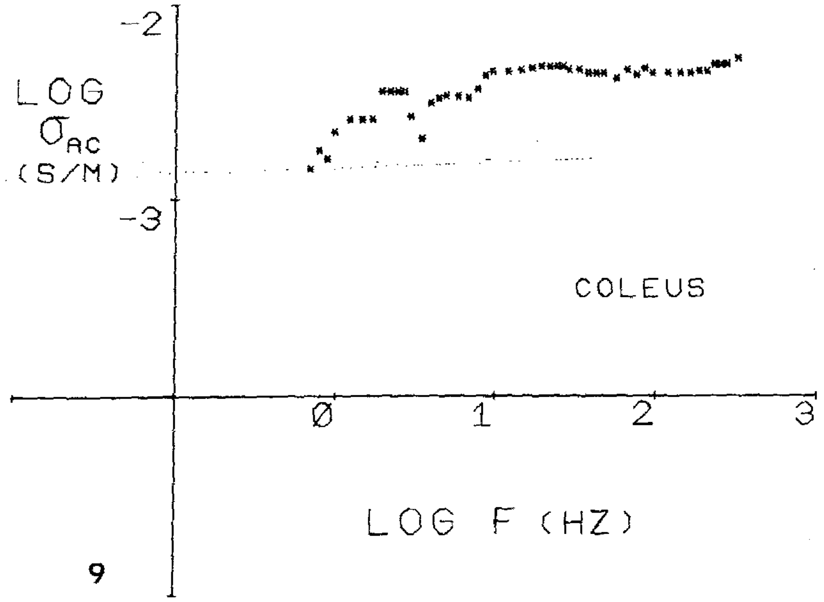

9

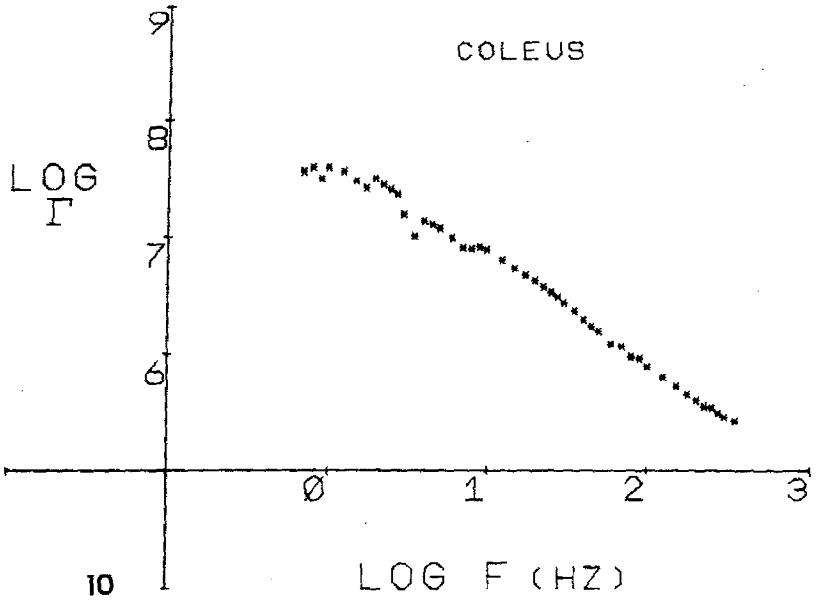

10

Fig. 9. Variation of stem AC conductivity with frequency for Coleus. The ordinate scale is logarithmic.
Fig. 10. Variation of stem dielectric loss with frequency for Coleus. The ordinate scale is logarithmic.

It is reasonable to expect that the dielectric response of plant stems should be ionic in nature. Conduction should take place primarily through the phloem and xylem, which can be approximated in herbaceous stems as one-dimensional channels. The present results can be compared with those taken from the data obtained for bone in the longitudinal direction [Lakes et al, 1977] and for hollandites [Jonscher, 1978]. For both of these the conduction is also ionic and essentially one-dimensional. For both materials the dielectric constant in the ELF range can be expressed according to equation 8 with $p_1 > p_2$ and $K_1 > K_2$. Moreover, for these materials the dielectric loss decreases smoothly with frequency in this range with no apparent peak. Such results are expected for ionic conductors [Jonscher, 1978; Hill and Jonscher, 1983].

More detailed comparison of the dielectric properties of plant stems with other biomaterials and with inorganic materials requires further experimentation over a wider frequency range and with a greater variety of plants. For example it would be of interest to compare the dielectric properties of woody stems, which might be approximated as two-dimensional channels, with the beta aluminas. Continued agreement of the observed dielectric properties of biomaterials with the cooperative response models could lead to an understanding of nonthermal bioeffects as being the result of the very low energy excitation of correlated states in the surrounding materials by the coupled ionic carriers.

ACKNOWLEDGMENTS

I would like to express my appreciation to Dr. Cyril Smith of the University of Salford in whose laboratory the experimental work was carried out, and to Drs. Robert Hill and Leonard Dissado of Chelsea College, University of London, for helpful discussions.

REFERENCES

Bean RC, Rasor JP, Porter GC (1960): Changes in the electrical characteristics of avocados during ripening. Yearb Calif Avocado Soc 44:75–78.

Broadhurst M (1970): Complex dielectric constant and dissipation factor of foliage. Natl Bur Stand Rep 9592. Springfield VA: National Technical Information Service.

Dissado LA, Hill RM (1979): Non-exponential decay in dielectrics and dynamics of correlated systems. Nature 279:685–689.

Edwards DF (1980): Proposed instrumentation to determine the optimum time to inseminate cattle by measurement of vaginal impedance. Med Biol Eng Comput 18:73–80.

Gensler W (1974): Bioelectric potentials and their relation to growth in higher plants. Ann NY Acad Sci 238:281–299.

Hart FX (1982a): Some precautions in the use of time-domain dielectric spectroscopy with biological and other lossy dielectrics. Med Biol Eng Comput 20:401–407.

Hart FX (1982b): The use of time domain dielectric spectroscopy to characterize the progress of wound repair. J Bioelect 1:313–328.

Hart FX (1983a): Changes in the dielectric properties of a plant stem produced by the application of voltage steps. Int J Biometeor 27:29–40.

Hart FX (1983b): Time domain dielectric spectroscopy of plant stems. Conference on Electrical Insulation and Dielectric Phenomena; Buck Hills Falls, PA; Oct 16–20, 1983. New York: IEEE, pp 391–396.

Hart FX (1984): Further precautions in the use of time domain dielectric spectroscopy with biological and other lossy dielectrics. Med Biol Eng Comput 22:379–381.

Hill RM, Jonscher AK (1983): The dielectric behaviour of condensed matter and its many-body interpretation. Contemp Phys 24:75–110.

Jonscher AK (1978): Low-frequency dispersion in carrier-dominated dielectrics. Phil Mag B 38:587–601.

Jonscher AK (1981): A new understanding of the dielectric relaxation of solids. J Mater Sci 16:2037–2060.

Kirk RE (1978): "Introductory Statistics." Monterey, CA: Brooks/Cole.

Lakes RL, Harper RA, Katz JL (1977): Dielectric relaxation in cortical bone. J Appl Phys 48:808–811.
Ngai KL, White CT (1979): Frequency dependence of dielectric loss in condensed matter. Phys Rev B 20:2475–2486.
Singh B, Smith CW, Hughes R (1979): In vivo dielectric spectrometer. Med Biol Eng Comput 17:45–60.
Young K (1982): Effect of low-frequency modes on dielectric loss in solids. Phys Rev B 25:2899–2904.